

# Electronic structure of praseodymium monpnictides and monochalcogenides under pressure

G Vaitheeswaran<sup>1,4</sup>, L Petit<sup>2,3</sup>, A Svane<sup>3</sup>, V Kanchana<sup>1,4</sup> and M Rajagopalan<sup>1</sup>

<sup>1</sup> Department of Physics, Anna University, Chennai 600 025, India

<sup>2</sup> Computer Science and Mathematics Division, and Center for Computational Sciences,

Oak Ridge National Laboratory, Oak Ridge, TN 37831-6114, USA

<sup>3</sup> Department of Physics and Astronomy, University of Aarhus, DK-8000 Aarhus C, Denmark

E-mail: g.s.vaithee@fkf.mpg.de

Received 15 April 2004

Published 11 June 2004

Online at [stacks.iop.org/JPhysCM/16/4429](http://stacks.iop.org/JPhysCM/16/4429)

doi:10.1088/0953-8984/16/25/004

## Abstract

The electronic structure of the praseodymium monpnictides and monochalcogenides is studied using the self-interaction corrected (SIC) local spin density (LSD) approximation. This method allows for a description of the Pr ions with some f electrons localized in atomic like orbitals, while other f degrees of freedom are forming hybridized bands. In this way different valency configurations of the Pr ion may be compared. The ground state configuration is obtained from the global energy minimum. With trivalent Pr ions, corresponding to two localized f electrons per Pr ion, the experimental lattice constants and bulk moduli of all these compounds are well reproduced. In contrast, the conventional LSD band treatment of the Pr pnictides and chalcogenides yields too small lattice constants. With applied pressure, the Pr monpnictides and monochalcogenides undergo simple B1 to B2 structural transitions which are well reproduced by the present theory without destabilization of the localized f<sup>2</sup> shells.

## 1. Introduction

There is a growing interest in the study of rare-earth pnictides and chalcogenides. Despite their simple rock-salt structure [1], they exhibit large variety in magnetic and electronic properties. Recently, the interest in these materials has further increased after it was demonstrated that they can be grown epitaxially on III–V semiconductors [2]. This opens up the way for the development of electronic devices such as metal base transistors. Praseodymium chalcogenides have attracted considerable attention due to their potential application for hyperfine enhanced nuclear cooling and the study of combined electron and nuclear ordering phenomena at very

<sup>4</sup> Present address: Max-Planck-Institut für Festkörperforschung, 70569 Stuttgart, Germany.

low temperatures [3]. From the theoretical point of view, the electronic properties of the rare-earth compounds are mainly determined by the degree of localization of the 4f electrons, the treatment of which presents a considerable challenge to band theory. The classification of the rare earths and their compounds in terms of their valencies provides an elementary explanation of their physical properties. In particular, changes in the lattice parameter of the rare earths can be related to valency change [4]. Praseodymium is the neighbour of cerium in the periodic table of the elements and some of the peculiar properties which are encountered in cerium and its compounds do also occur in praseodymium. The present study of Pr monopnictides and monochalcogenides aims at shedding more light on the properties of these systems.

Several experimental and theoretical studies on the electronic structure and high pressure behaviour of rare-earth monopnictides and monochalcogenides have been published. In the lanthanum monopnictides a pressure induced structural phase transition occurs from the NaCl (B1) structure to a tetragonal structure, which may be viewed as a distorted CsCl (B2) structure. In the lanthanum monochalcogenides similar phase transitions were predicted to occur, however to a pure B2 phase. Recent studies of the electronic structure of the lanthanum monopnictides [5, 6] and monochalcogenides [7], using the self-consistent tight-binding linear muffin-tin orbital (LMTO) method, confirm the observed behaviour of these materials under pressure. From Ce onwards, the presence of localized f electrons makes a similar band structure calculation inadequate, as the LSD approximation does not capture the strong correlation effects. In the LDA + *U* method, the position of the narrow f bands is corrected by explicitly including these correlations. The method has been applied to calculate the electronic structure and optical properties of the Pr pnictides [8]. A second approach treats the f electrons as part of the core, whilst the remaining valence electrons continue to be treated in the LSD approximation. This method was among others applied to RESb compounds [9], and Gd, and Er pnictides [10]. In the present work we will undertake a systematic theoretical investigation of the Pr monopnictides and monochalcogenides using an *ab initio* electronic structure method based on the self-interaction corrected (SIC) local spin density (LSD) approximation [11]. In this scheme the Pr f electrons may be described as either localized or delocalized, and various valencies of Pr can be investigated and the most favourable predicted.

The SIC-LSD method has previously been successfully applied to the electronic structure of divalent and trivalent rare-earth sulfides [12, 13]. Also, extensive theoretical studies on the electronic structure and high pressure behaviour of Ce pnictides and chalcogenides [14, 15] were carried out using the SIC-LSD approximation, and a B1 to B2 structural phase transition was demonstrated to occur in conjunction with a localized to delocalized transition of the f electrons. Here we use this same approach to investigate the effects of pressure on the relative stability of the B1 and B2 phases of Pr pnictides and chalcogenides. The PrX compounds behave similarly to the LaX and CeX compounds. Their high pressure behaviour, up to 40 GPa, was studied extensively using synchrotron radiation. Experimental studies on PrP [16] reveal a crystallographic transition from B1 to a tetragonal structure (distorted B2) around 26 GPa with a volume collapse of 12.1%. Similar structural transitions were observed in PrAs [17], PrSb [18] and PrBi [19] with transition pressures of 27, 13 and 14 GPa, respectively. Experimental studies of the high pressure behaviour of PrTe [20] report a simple B1 to B2 structural transition around  $9 \pm 1$  GPa with a volume reduction of 11.5%. No pressure experiments have been reported for PrS and PrSe.

The remainder of the paper is organized as follows. In the next section, we briefly present the theoretical background of the SIC-LSD approach. In section 3 our results of the structural studies of Pr monopnictides and monochalcogenides are compared to experiment. In section 4 the electronic band structure and density of states of these compounds are discussed in detail. The final section is devoted to conclusions.

## 2. SIC-LSD formalism

The basis of the SIC-LSD formalism is a self-interaction free total energy functional  $E^{\text{SIC}}$ , obtained by subtracting from the LSD total energy functional  $E^{\text{LSD}}$  the self-interaction of each occupied electron state  $\psi_\alpha$  [21]:

$$E^{\text{SIC}} = E^{\text{LSD}} - \sum_{\alpha}^{\text{occ}} \delta_{\alpha}^{\text{SIC}}. \quad (1)$$

Here, the self-interaction correction for the state  $\psi_\alpha$  is

$$\delta_{\alpha}^{\text{SIC}} = U[n_{\alpha}] + E_{\text{XC}}^{\text{LSD}}[n_{\alpha}] \quad (2)$$

with  $U[n_{\alpha}]$  being the Hartree energy and  $E_{\text{XC}}^{\text{LSD}}[n_{\alpha}]$  the LSD exchange–correlation energy for the corresponding charge density  $n_{\alpha} = |\psi_{\alpha}|^2$ . It is the LSD approximation to the exchange–correlation energy functional which gives rise to the spurious self-interaction. The exact exchange–correlation energy of density functional theory,  $E_{\text{XC}}$ , has the property that for any single electron spin density,  $n_{\alpha}$  it cancels exactly the Hartree energy [21]:

$$U[n_{\alpha}] + E_{\text{XC}}[n_{\alpha}] = 0. \quad (3)$$

In the LSD approximation this cancellation is incomplete, and for spatially well localized states  $\psi_{\alpha}$  the self-interaction  $\delta_{\alpha}$  can be substantial. On the other hand, for extended states in periodic solids the self-interaction vanishes. Hence, in order to gain energy from the self-interaction correction in a periodic solid, the Bloch symmetry of the wavefunction  $\psi_{\alpha}$  must be broken. This does not conflict with Bloch’s theorem, since the Hamiltonian describing the state  $\psi_{\alpha}$  will no longer be translationally invariant [22]. For a full exploration of the functional in equation (1), various scenarios of localized and delocalized states need to be examined. The LSD minimum remains a local minimum of  $E^{\text{SIC}}$ , since the scenario with no localized states is a viable option, but other scenarios may result in a lower total energy, as is indeed found in Pr compounds in this work. The localized electrons acquire core like characteristics, and the self-interaction correction plays the role of localization energy which competes with the band formation energy gained by allowing electrons to delocalize. The number of localized f electrons leads to a convenient definition of the valency of the rare-earth ion [12], given as the number of electrons available for band formation:

$$N_{\text{val}} = Z - N_{\text{core}} - N_{\text{SIC}}. \quad (4)$$

Here  $Z$  (=59) is the atomic number,  $N_{\text{core}}$  is the number of the atomic core (and semi-core) electrons (=54 for Pr) and  $N_{\text{SIC}}$  is the number of localized f electrons. Thus, with two localized f electrons ( $f^2$ ) the Pr ion will be trivalent. Similarly,  $f^1$  and  $f^0$  configurations would be referred to as tetravalent and pentavalent configurations. It is important to note that those f degrees of freedom which are not localized are available for band formation. The pentavalent configuration corresponds to the normal LSD picture, i.e. the entire f manifold is treated as band states. The SIC-LSD approach [22] has been implemented with the LMTO method [23]. The atomic sphere approximation (ASA) is used, according to which the polyhedral Wigner–Seitz cell is approximated by slightly overlapping atom centred spheres. The spin–orbit interaction is included explicitly in the Hamiltonian [24]. To improve packing in the NaCl structure, ‘empty spheres’ have been introduced in the high symmetry interstitial sites [25]. Since the ASA is not sufficiently accurate for calculating the energy difference between the NaCl and CsCl structures, we have used the full potential (FP) LMTO method [26] to correct the ASA total energies, i.e. we assume that the LSD total energy correction between the FP and ASA (at a particular lattice constant) can be taken over also to SIC-LSD calculations. The calculations used 525 and 455  $k$  points in the irreducible Brillouin zone of the NaCl and CsCl structures,

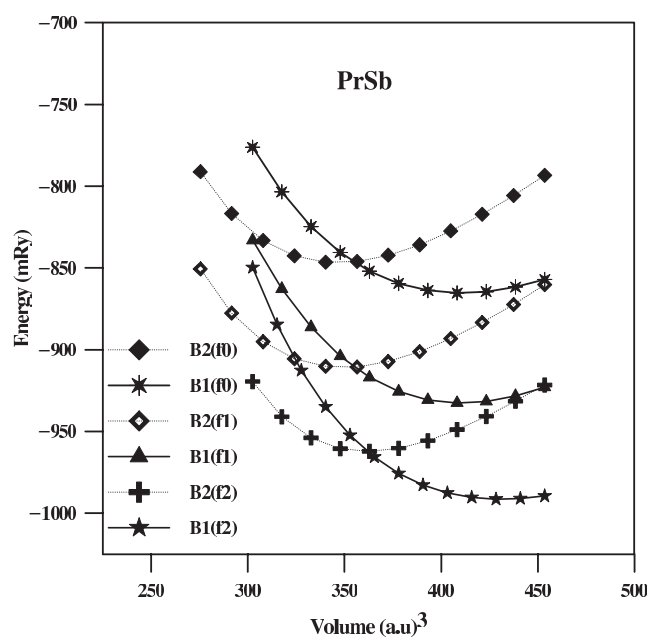


**Figure 1.** Calculated total energy versus relative volume of PrSb in the B1 and B2 structures with the Pr ions in the trivalent, tetravalent and pentavalent configurations.  $V_0 = 432 \text{ au}^3$ .

respectively. The inclusion of Pr 5p states as band states (in a separate semi-core panel) is crucial for getting an accurate evaluation of the total energy. Apart from those f states that remain delocalized, the valence panel contains the Pr 6s and 5d states, as well as the pnictide/chalcogenide s, p and d states.

### 3. Structural studies

The results of the present structural calculations are presented in figures 1–4 with the numerical details compiled in tables 1–3. In all of the calculations presented in this section a ferromagnetic alignment of Pr moments is assumed. The result of our total energy calculations is that for all PrX compounds the ground state is found in the B1 structure with two localized f electrons on Pr. Thus, it can be seen from column 2 of table 1 that in the B1 structure the  $f^2$  configuration is energetically favoured over the  $f^1$  configuration, and from column 3 we find that B1 structure is always favoured with respect to the B2 structure. Treating the f electrons as localized (column 5) instead of as band states (column 4) leads to higher values of the equilibrium lattice constants which are in better agreement with experimental values (column 6).

#### 3.1. Praseodymium pnictides

The total energies as a function of relative volume are calculated for all the Pr pnictides for both the B1 and B2 phases, and in three valency scenarios, i.e. with either two, one or zero localized f electrons per Pr atom, corresponding respectively to the trivalent, tetravalent and pentavalent configurations. The lowest energy is reached in the B1 phase with two localized f electrons. In PrP the calculated equilibrium lattice constant is 11.13 au, which deviates only 0.2% from the experimental value. The calculated bulk modulus is 70 GPa which compares favourably to the experimental value of  $74 \pm 2$  GPa [19]. Under pressure, PrP undergoes a structural transition from B1 to B2 around 16 GPa, accompanied by a volume reduction of 13.1%, whereas the experimental structural transition to distorted B2 is found to be at 26 GPa [16].

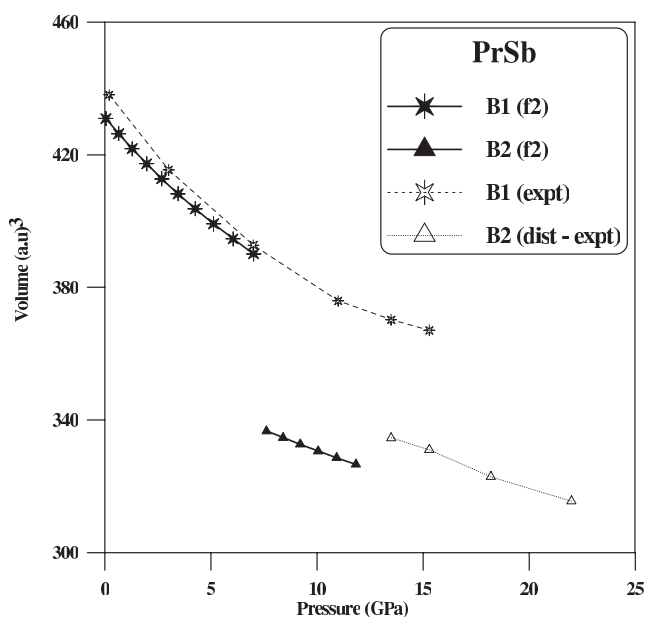


**Figure 2.** The calculated pressure–volume curve for PrSb in the B1 and B2 phases with the Pr ions in the trivalent configuration. Experimental points [18] for the B1 and distorted B2 phase are included for comparison.

**Table 1.** Calculated energy differences between the trivalent and tetravalent Pr ion configurations in PrX compounds in the B1 structure (in mRyd per Pr). Also shown are the energy differences of the B1 and B2 structures with trivalent Pr ions (likewise in mRyd per Pr), and the B1 lattice constants,  $a$  (in au), for itinerant  $f$  electrons (pentavalent Pr ions) and for trivalent Pr (localized  $f^2$  shells). The last column gives the experimental lattice constants.

Compound	$E(f^2) - E(f^1)$ (mRyd)	$E(B1) - E(B2)$ (mRyd)	$a(f^0)$	$a(f^2)$ (au)	$a(\text{Expt})$
PrP	−48.5	−46.1	10.87	11.13	11.15 [16]
PrAs	−53.3	−36.6	11.06	11.43	11.34 [17]
PrSb	−59.5	−26.3	11.79	11.99	12.00 [18]
PrBi	−62.2	−25.8	11.99	12.14	12.21 [27]
PrS	−48.2	−47.1	10.66	10.86	10.83 [27]
PrSe	−52.3	−28.7	11.10	11.26	11.23 [27]
PrTe	−54.2	−12.0	11.75	11.92	11.93 [27]

The equilibrium lattice constant of PrAs is calculated to be 11.43 au, which is slightly higher than the experimental value. The bulk modulus is calculated to be 64 GPa while the experimental value is anomalously high at  $100 \pm 7$  GPa. Like PrP, PrAs undergoes a structural transition from B1 to B2 calculated to occur at 12 GPa with a volume collapse of 13.7%. This is to be compared to the B1  $\rightarrow$  B2 (distorted) phase transition observed experimentally at 27.1 GPa with a volume collapse around 9% [19]. The total energy as a function of volume of PrSb is shown in figure 1. As mentioned earlier, three valency scenarios are depicted for the B1 and B2 structures. The calculated lattice constants in the B1 phase with the trivalent ground state configuration is found to be in excellent agreement with experiment. The calculated bulk modulus is 55 GPa for PrSb which is somewhat higher than the experimental values  $44 \pm 5$  GPa. Like PrP and PrAs, PrSb also undergoes a transition from B1 to B2 around 8 GPa, with a volume collapse of 13%. The theoretical  $p(V)$  curve is shown in figure 2. Experimentally [18], PrSb undergoes a structural transition to a distorted B2 phase around 13 GPa. The  $c/a$  ratio of the distorted phase is 0.82. Like studies of Ce pnictides [14], FP-

**Table 2.** Calculated and experimental bulk moduli (in GPa) of Pr monopnictides and monochalcogenides in the NaCl structure. The calculations are for the ground state with two localized f electrons on Pr.

Compound	Theory	Expt
PrP	70	74 ± 2 [19]
PrAs	64	100 ± 7 [19]
PrSb	55	44 ± 5 [19]
PrBi	51	40 ± 5 [19]
PrS	89	107 [28]
PrSe	78	92 [28]
PrTe	57	—

**Table 3.** Calculated and experimental transition pressures,  $P_t$  (in GPa), and volume changes (in %), for the B1 → B2 structural phase transition of the Pr monopnictides and monochalcogenides.

Compound	$P_t$		$V_1/V_0$		$V_2/V_0$	
	Theory	Expt	Theory	Expt	Theory	Expt
PrP	16	26 [19]	0.865	—	0.751	—
PrAs	12	27 [19]	0.902	0.903 [19]	0.778	0.719 [19]
PrSb	8	13 [19]	0.896	0.870 [19]	0.779	0.770 [19]
PrBi	8	14 [19]	0.873	0.875 [19]	0.764	0.785 [19]
PrS	22	—	0.843	—	0.763	—
PrSe	12	—	0.891	—	0.798	—
PrTe	5	9 ± 1 [20]	0.928	—	0.811	—

LMTO studies in the LSD approximation find the undistorted and distorted B2 structures very close in energy, so the use of undistorted B2 phase in the comparison to experiment should not be a too serious approximation. The experimental volume collapse is  $\Delta V/V_0 = 12.1\%$ , which is in excellent agreement with the theoretical value of 13%. From figure 1 we see that the phases with fewer localized f electrons, the tetravalent and pentavalent phases, have a higher energy and are thus not relevant, except at very high pressures in the 50–100 GPa range.

Finally, for PrBi we also find the theoretical lattice constant in the trivalent ground state configuration to be in excellent agreement with experiment. The calculated bulk modulus is 51 GPa, which is somewhat higher than the experimental value,  $40 \pm 5$  GPa. We find a B1 (trivalent) to B2 (trivalent) phase transition taking place at 8 GPa, with a volume collapse of around 12.5%. Experimentally, around 14 GPa, PrBi is found to undergo a structural transition into what appears as a coexisting pure B2 and distorted B2 phase [19]. The volume collapses are quite similar in theory and experiment.

The present theory thus provides a picture in very good agreement with the experimental results. For the transition pressures we observe that our values are consistently below the experimental ones. We also notice that for PrSb and PrBi, these values are in slightly better agreement with experiment than is the case for PrP and PrAs.

### 3.2. Praseodymium chalcogenides

The total energy as a function of relative volume for PrS is shown in figure 3, again considering both the B1 and B2 structures with trivalent, tetravalent and pentavalent Pr configurations. The lowest lying curve corresponds to the B1 phase of PrS in the trivalent configuration. The calculation predicts a structural transformation from B1 to B2 around 22 GPa with the Pr

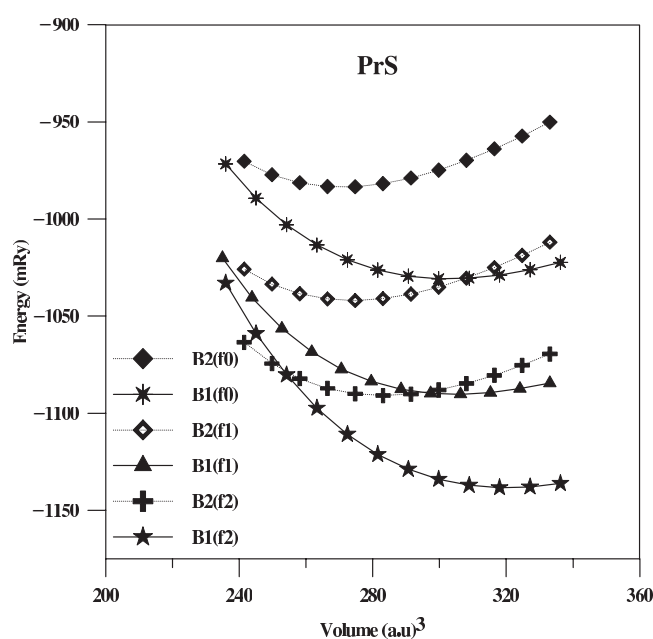


**Figure 3.** Calculated total energy versus relative volume of PrS in the B1 and B2 structures with the Pr ions in the trivalent, tetravalent and pentavalent configurations.  $V_0 = 317 \text{ au}^3$ .

ions remaining in their trivalent configuration. The accompanying volume collapse is 10% (figure 4). The energies of the tetravalent and pentavalent scenarios are higher and hence we conclude that the delocalization of the f shell does not occur for PrS at least for pressures up to 50 GPa. Additionally, the divalent scenario has also been tested for PrS, i.e. assuming localized  $f^3$  shells on Pr, but this configuration is almost 100 mRyd higher in energy than the trivalent configuration. It is interesting to compare the high pressure behaviour of PrS to that of the neighbouring compound CeS [15] and LaS [7]. In the case of CeS, the high pressure transition occurs in two steps. Firstly, an isostructural transition within the B1 structure occurs, at a theoretical pressure of 10.1 GPa, while experiment at room temperature finds the transition to be continuous. At this transition, the single f electron of Ce delocalizes and Ce changes from trivalent to tetravalent. Subsequently, at a pressure of 24.3 GPa, a transition from B1 to B2 occurs, with the Ce ions remaining tetravalent. For PrS, the present calculation thus finds the trivalent configuration to be more stable than in CeS. The calculated transition pressure of PrS is 22 GPa, i.e. comparable with the recent theoretical prediction of a B1 to B2 transition in LaS around 24 GPa [7]. There are no experimental high pressure studies reported for PrS, but as discussed, the neighbouring PrP compound undergoes a structural transformation from B1 to B2 (distorted) around 26 GPa [16].

For PrSe, the calculations similarly find a structural transformation from B1 to B2 to occur around 12 GPa with a volume collapse of 10.3%. As for PrS, the Pr ions remain trivalent across the transition. Also in the case of PrSe, we find no experimental results regarding the structural transitions under pressure. The PrSe calculations can be compared with the isostructural compounds LaSe and CeSe, for which similar B1 to B2 transitions occur at 12.7 [15] and 12.4 GPa [7], respectively, in the latter case with localized  $f^1$  Ce ions. The transition pressure of PrSe is significantly lower than that found for PrAs, where it is observed around 27.1 GPa [17].

In PrTe a similar B1 to B2 transition with trivalent Pr ions is found to occur at 5 GPa. The volume collapse associated with the transition is 12%. The transition pressure agrees quite

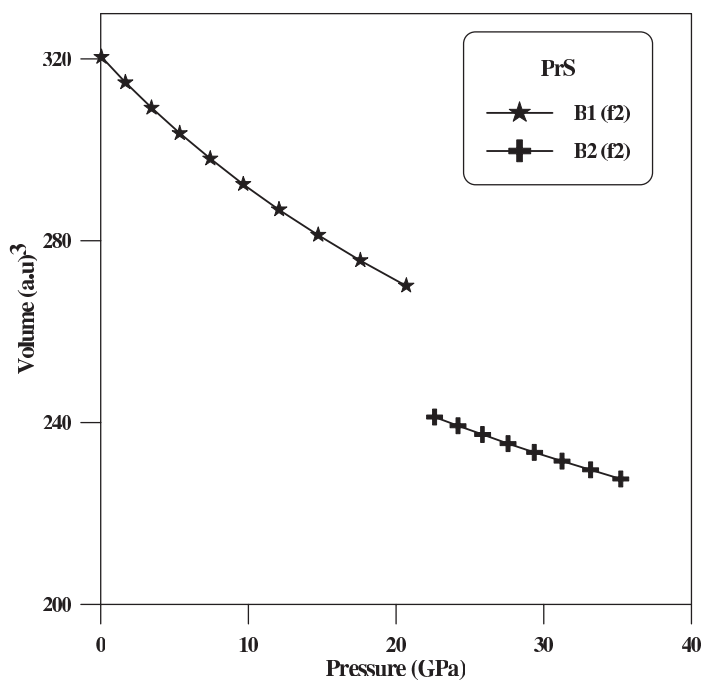


**Figure 4.** The calculated pressure–volume curve for PrS in the B1 and B2 phases with the Pr ions in the trivalent configuration.

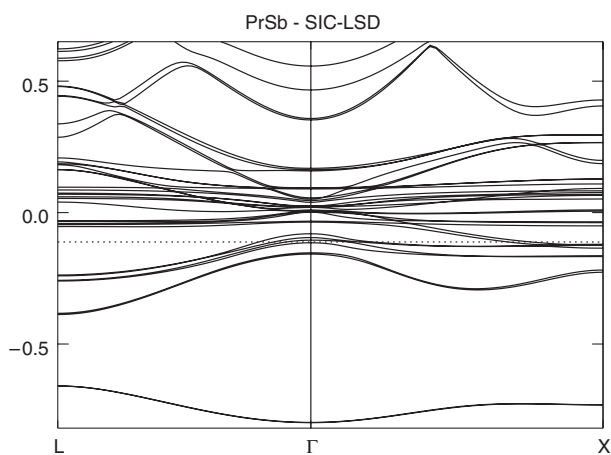


**Figure 5.** The band structure of PrSb in the trivalent configuration, i.e. with two localized f electrons on each Pr ion. The dotted line marks the Fermi level.

well with the experimental study [20], which observed the transition occurring at  $9 \pm 1$  GPa. In CeTe, a similar transition from B1 ( $f^1$ ) to B2 ( $f^1$ ) is calculated to occur around 7.4 GPa [15]. As for PrS and PrSe, the transition pressure for PrTe also differs markedly from the neighbouring pnictide PrSb, where a B1 to B2 (distorted) structural transition occurs at a pressure of around 13 GPa [18]. The observed high pressure phase of PrTe is pure B2. The calculated lattice parameter in the B1 phase is in excellent agreement with the experimental value and the calculated bulk modulus is 57 GPa.

In summary, the Pr chalcogenides undergo structural phase transitions at somewhat lower pressures than their corresponding pnictides. The Pr ion remains in the trivalent configuration through the transition.

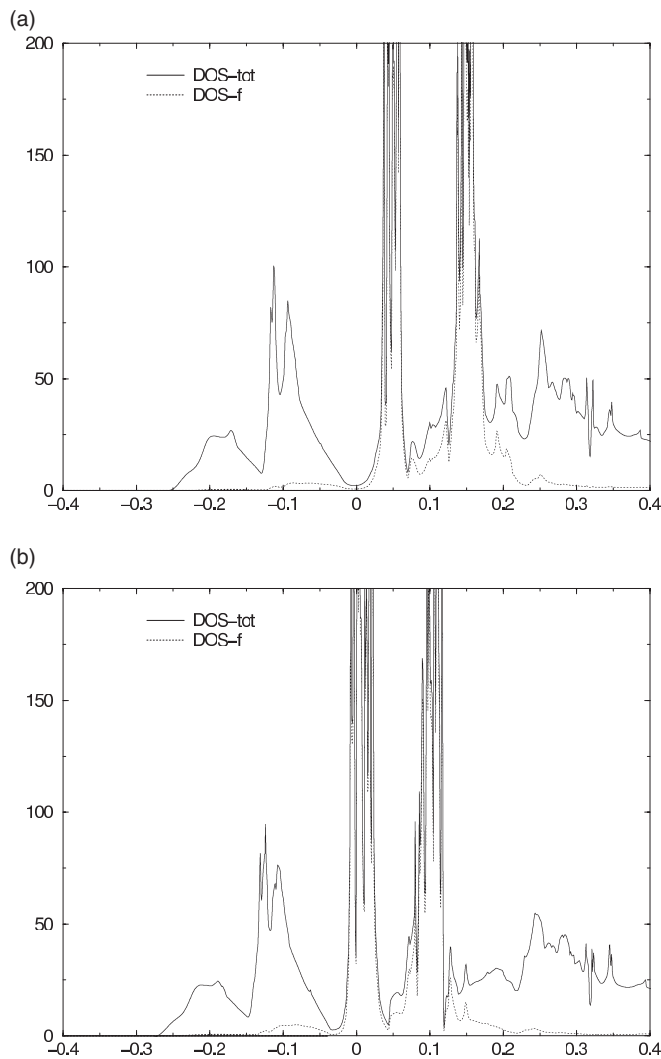


**Figure 6.** Densities of states of PrSb in (a) the trivalent and (b) the pentavalent configurations. Energy (in Ryd relative to the Fermi level) is plotted along the  $x$ -axis and the DOS (in units of states  $\text{Ryd}^{-1}$  per formula unit) along the  $y$ -axis. The full curve is the total DOS, while the dotted curve gives the itinerant Pr  $f$  partial DOS.

## 4. Band structure and density of states

### 4.1. Pr monpnictides

The calculated band structure and densities of states (DOS) of PrSb are shown in figures 5 and 6(a), assuming Pr to be in the trivalent ground state configuration, while figure 6(b) depicts the DOS assuming pentavalent Pr ions. The lowest lying valence band, around  $-0.6$  Ryd relative to the Fermi level, is mainly due to the Sb  $s$  state, which is well separated from the remaining valence bands. The rest of the valence bands are the Sb  $p$  bands which are highly hybridized with Pr  $s$  and  $d$  states which agrees well with the photoemission results [31]. The cluster of bands which are situated  $0.0$ – $0.2$  Ryd above the Fermi level are the itinerant  $f$  like states of Pr. PrSb remains metallic, as hole pockets in the vicinity of the  $\Gamma$  point compensate electron pockets around the  $X$  points. The major contribution to the density of states at the Fermi level comes from the  $d$  states of Pr and the  $p$  states of Sb. The calculated total DOS at the Fermi level is rather low, as can be seen from figure 6(a). The two peaks situated

below the Fermi level can be observed as the broad hybridized spd bands. With respect to the f bands, we notice some hybridization with the spd band, but the main part is bundled in the two large, exchange split peaks, above the Fermi level. The two f electrons that are localized in the trivalent configuration are not shown in the DOS plot. In the pentavalent scenario no f electrons are self-interaction corrected but all are allowed to hybridize with the valence band. This corresponds to the normal LSD picture and, as seen from figure 6(b), results in a significantly different DOS at the Fermi level. The additional delocalized f states lead to a higher density of states at the Fermi level, which is now situated inside the itinerant f peak. As noted earlier, all the Pr pnictides prefer the trivalent ground state configuration, and their DOS are therefore very similar to that for PrSb. More specifically they all have a very low DOS at the Fermi level, which leads to the classification of these systems as low carrier systems. With decreasing size of the pnictide ion the direct f–f overlap increases, and the hybridization of Pr f and pnictogen p becomes more significant.

#### 4.2. *Pr monochalcogenides*

The calculated density of states of PrS, in the B1 structure and assuming the trivalent ground state configurations of Pr, is shown in figure 7(a). The valence band consists mainly of the S sp bands which strongly hybridize with Pr s and d states. Comparing to the DOS of PrSb in figure 6(a), one notices the lowering of the ligand p bands with respect to the Pr derived s and d states, which is due to the increased attraction to the nucleus, when going from the pnictide to the chalcogenide. The key point to note is the position of the unoccupied f states relative to the Fermi energy, and the small occupied tail of this peak below the Fermi energy. Compared to the case for the pnictides, the contribution of the f states at the Fermi level is now considerably larger, and overall one obtains a non-negligible DOS at the Fermi level. The main reason for this difference is that in the pnictide atom, the p orbital is only half-filled, and can accommodate three electrons from Pr which, combined with the localization of two f electrons, results in an almost vanishing DOS at the Fermi level. In the chalcogenides, on the other hand, only two p orbitals are unoccupied and, for combination with Pr, two sd electrons together with the p electrons fill this band, with no space left to accommodate the third Pr valence electron. Instead it fills the fd band up to the Fermi energy. A similar situation is observed for example in the actinide chalcogenides and pnictides [29]. A systematic comparison of the chalcogenides shows that as the chalcogen size increases from PrS to PrTe, the p orbitals are less tightly bound to the nucleus, i.e. in the solid, the p like states move towards the Fermi level and, as a consequence, the DOS at the Fermi level increases.

The DOS of PrS in the high pressure B2 structure is depicted in figure 7(b). Comparing with the B1 structure in figure 7(a), the f states contribute more towards the valence band in the B2 phase, where the Pr–Pr distance is considerably smaller. Hence the Pr f–f overlap is larger, leading to broader bands.

### 5. Conclusion

Calculations of the electronic structures of Pr monopnictides and monochalcogenides based upon the SIC-LSD approach have been presented. This is the first electronic structure calculation reported for Pr monopnictides and monochalcogenides where the localization of Pr f electrons is treated correctly. The Pr f electrons are described in a picture of coexisting localized and delocalized states. Each f electron can be treated as either localized or delocalized, which introduces an extra degree of freedom into the electronic structure calculations. The self-interaction correction in this approach provides a localization energy for the f electron, which competes with the hybridization energy gained upon delocalization of the f electron. The

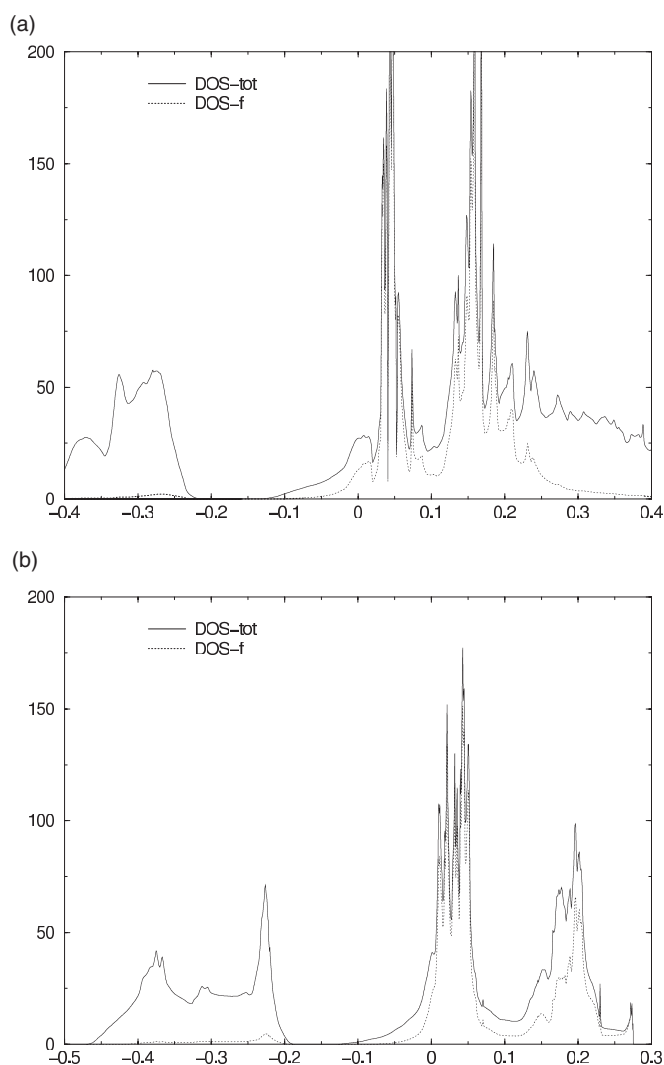


**Figure 7.** Densities of states of PrS in (a) the trivalent B1 and (b) the trivalent B2 configurations ( $V/V_0 = 0.89$ ). Energy (in Ryd relative to the Fermi level) is plotted along the  $x$ -axis and the DOS (in units of states  $\text{Ryd}^{-1}$  per formula unit) along the  $y$ -axis. The full curve is the total DOS, while the dotted curve gives the itinerant Pr  $f$  partial DOS.

concept of valency is introduced as the number of band forming valence electrons of Pr. Hence, this definition of valency refers to the appropriate form of the wavefunction of the Pr  $f$  electrons in the solid state environment, rather than to a change of character from  $f$  to non- $f$  character. The calculations have shown that the trivalent Pr configuration is the ground state in all these compounds and remains stable even under pressure up to  $\sim 50$  GPa. The experimental data for the equilibrium lattice constant and bulk modulus are well reproduced by the calculation, demonstrating that the bonding properties of Pr monopnictides and monochalcogenides are accurately described by the SIC-LSD method. With applied pressure all these compounds undergo structural phase transitions to the CsCl structure (or a distorted version of it). The calculated transition pressures of Pr monopnictides agree quite well with the experimental results but are systematically lower. Also for the case of PrTe the calculated transition pressure agrees with the experimental value, while the predicted transitions for PrS and PrSe still await experimental confirmation. Unlike the case for the cerium pnictides and chalcogenides, the trivalent configurations of Pr in the Pr monopnictides and monochalcogenides are stable,

although elemental Pr is known to undergo a sequence of structural changes with applied pressure accompanied by increasing delocalization of the f states [30]. The present calculations find the PrX compounds to be all metallic with the density of states at the Fermi level increasing from PrP to PrBi and also from PrS to PrTe.

### Acknowledgments

This work was partially funded by the EU TMR Networks (contracts: FMRX-CT98-0178 and HPRN-CT-2002-00295). Support from the Danish Centre for Scientific Computing is acknowledged. The work of L Petit is supported in part by the Defense Advanced Research Project Agency, and by the Division of Materials Science and Engineering, US Department of Energy, under contract No DE-AC05-000R22725 with UT-Battelle LLC. The author VK acknowledges CSIR India for financial support. The authors GV and VK also acknowledge Professor I Shirovani, Muroran Institute of Technology, Japan, for providing experimental results prior to publication.

### References

- [1] Hülliger F 1979 *Handbook on the Physics and Chemistry of Rare Earths* vol 4, ed K A Gschneidner Jr and L Eyring (Amsterdam: North-Holland) p 153
- [2] Allen S J, Brehmer D and Palmstrom C J 1993 *Rare Earth Doped Semiconductors* vol 301, ed G S Pomrenka, P B Klein and D W Langer (Pittsburg, PA: Materials Research Society) p 307
- [3] Andres K and Bucher E 1971 *J. Appl. Phys.* **42** 1522
- [4] Jayaraman A 1979 *Handbook on the Physics and Chemistry of Rare Earths* vol 1, ed K A Gschneidner Jr and L Eyring (Amsterdam: North-Holland) chapter 9
- [5] Vaitheeswaran G, Kanchana V and Rajagopalan M 2002 *J. Alloys Compounds* **336** 46
- [6] Vaitheeswaran G, Kanchana V and Rajagopalan M 2002 *Physica B* **315** 64
- [7] Vaitheeswaran G, Kanchana V and Rajagopalan M 2003 *J. Phys. Chem. Solids* **64** 16
- [8] Ghosh D B, De M and De S K 2003 *Phys. Rev. B* **67** 035118
- [9] Norman M R, Koelling D D and Freeman A J 1985 *Phys. Rev. B* **32** 7748
- [10] Petukhov A G, Lambrecht W R L and Segall B 1996 *Phys. Rev. B* **53** 4324
- [11] Svane A and Gunnarsson O 1990 *Phys. Rev. Lett.* **65** 1148
- [12] Strange P, Svane A, Temmerman W M, Szotek Z and Winter H 1999 *Nature* **399** 756
- [13] Temmerman W M, Svane A, Strange P, Szotek Z and Winter H 2000 *Phil. Mag.* **B 80** 1179
- [14] Svane A, Szotek Z, Temmerman W M, Laegsgaard J and Winter H 1998 *J. Phys.: Condens. Matter* **10** 5309
- [15] Svane A, Temmerman W and Szotek Z 1999 *Phys. Rev. B* **59** 7888
- [16] Adachi T, Shirovani I, Hayashi J and Shimomura O 1998 *Phys. Lett. A* **250** 389
- [17] Shirovani I, Yamanashi K, Hayashi J, Tanaka Y and Ishimatsu N 2001 *J. Phys.: Condens. Matter* **13** 1939
- [18] Hayashi J, Shirovani I, Tanaka Y, Adachi T, Shimomura O and Kikegawa T 2000 *Solid State Commun.* **114** 561
- [19] Shirovani I, Hayashi J, Yamanashi K, Hirano K, Adachi T, Ishimatsu N, Shimomura O and Kikegawa T 2003 *Physica B* **334** 167
- [20] Chatterjee A, Singh A K and Jayaraman A 1972 *Phys. Rev. B* **6** 2285
- [21] Perdew J P and Zunger A 1981 *Phys. Rev. B* **23** 5048
- [22] Svane A 1996 *Phys. Rev. B* **53** 4275
- [23] Andersen O K 1975 *Phys. Rev. B* **12** 3060
- [24] Nordström L, Wills J M, Andersen P H, Söderlind P and Eriksson O 2001 *Phys. Rev. B* **63** 035103
- [25] Glötzel D, Segall B and Andersen O K 1980 *Solid State Commun.* **36** 403
- [26] Methfessel M 1988 *Phys. Rev. B* **38** 1537
- [27] Wyckoff R W G 1972 *Crystal Structures* (New York: Plenum)
- [28] Morosin B and Schriber J E 1979 *Phys. Lett. A* **73** 50
- [29] Petit L, Svane A, Temmerman W M and Szotek Z 2001 *Phys. Rev. B* **63** 165107
- [30] Söderlind P 2002 *Phys. Rev. B* **65** 115105
- [31] Campagna M, Bucher E, Wertheim G K, Buchanon D N E and Longinotti D L 1974 *Proc. 11th Conf. on Rare-Earth (Trasverse City, MI, 1974)* ed J M Haschke and H A Eick (Springfield, VA: NTIS) p 810